Chemically fashioned ZnO nanowalls and their potential application for potentiometric cholesterol biosensor

M.Q. Israr, J.R. Sadaf, Omer Nur, Magnus Willander, S. Salman and B. Danielsson

Linköping University Post Print

N.B.: When citing this work, cite the original article.

Original Publication:

M.Q. Israr, J.R. Sadaf, Omer Nur, Magnus Willander, S. Salman and B. Danielsson, Chemically fashioned ZnO nanowalls and their potential application for potentiometric cholesterol biosensor, 2011, Applied Physics Letters, (98), 25, 253705.

http://dx.doi.org/10.1063/1.3599583

Copyright: American Institute of Physics

http://www.aip.org/

Postprint available at: Linköping University Electronic Press http://urn.kb.se/resolve?urn=urn:nbn:se:liu:diva-69852

Chemically fashioned ZnO nanowalls and their potential application for potentiometric cholesterol biosensor

M. Q. Israr, ^{1,a)} J. R. Sadaf, ¹ O. Nur, ¹ M. Willander, ¹ S. Salman, ² and B. Danielsson ^{2,3} ¹Department of Science and Technology, Campus Norrköping, Linköping University, SE-60174 Norrköping, Sweden

(Received 15 May 2011; accepted 18 May 2011; published online 22 June 2011)

Chemically fashioned zinc oxide (ZnO) nanowalls on aluminum wire have been characterized and utilized to fabricate a potentiometric cholesterol biosensor by an electrostatic conjugation with cholesterol oxidase. The sensitivity, specificity, reusability, and stability of the conjugated surface of ZnO nanowalls with thickness of ~ 80 nm have been investigated over a wide logarithmic concentrations of cholesterol electrolyte solution ranging from $1 \times 10^{-6} - 1 \times 10^{-3}$ M. The presented biosensor illustrates good linear sensitivity slope curve (~ 53 mV/decade) corresponding to cholesterol concentrations along with rapid output response time of ~ 5 s. © 2011 American Institute of Physics. [doi:10.1063/1.3599583]

The estimation of the cholesterol level in human body is significantly important for all animal cells and its functioning in the production of steroids and oxysterols hormones and bile acids. 1,2 However, the elevated cholesterol level could become a serious threat for living bodies in the form of pathogenesis of dementias, diabetes, cancer, cardiac, and brain vascular diseases and several rare monogenic diseases.³⁻⁶ The requirement of the controlled cholesterol level in human blood cells leads toward the development of efficient and robust cholesterol biosensors. Variety of materials is being investigated for the preparation of biosensors possessing good specificity, selectivity, and rapid output response. Among the diverse materials, zinc oxide (ZnO) is one of the most exciting contenders for the fabrication of facile, biosafe, reliable, and low cost biosensors. The plenteous nanoscale structures of ZnO owing to their large specific surface area and extraordinary electrical and thermal stabilities have become a center of attention of the researchers.^{7,8} Compatibility of ZnO nanostructures with biological species depending on their size and shape is highly influential for successful developments in the area of biosensors. Additionally, ZnO nanostructures hold a promising potential for the practical biosensing applications due to their excellent stability at neutral pH. 9-13 Immobilization of enzyme could further help to produce the highly stable, molecule specific and reusable biosensor and also, improves the output response time by utilizing its capabilities as a catalyst. Cholesterol oxidase (ChOx) enzyme is highly important constituent of cholesterol metabolism which can provide an extremely useful transducer for electrochemical biosensors. Diverse methods such as; covalent bonding, entrapment, and cross-linking etc. are being used to achieve the immobilization of negatively charged ChOx enzyme having lower isoelectric point onto ZnO possessing higher value of isoelectric point. 14-17 ZnO nanoscale structures e.g., rods, particles, and flowers etc. have aroused a substantial interest for their application as a cholesterol biosensor having large surface area to volume ratio, nontoxic and biological size-compatible characteristics.

Scanning electron microscopy (SEM) has been utilized to visualize the three dimensional quantitative analysis of ZnO nanowalls. Figure 1(a) depicts panoramic view of homogeneously grown ZnO nanowalls nearly perpendicular to the Al wire with an average thickness of ~80 nm while in insert a high magnified SEM image reveals a smooth and clear surface of ZnO nanowalls. Low-resolution transmission electron microscope (LRTEM) illustrates thin, smooth, and impurity free surface of nanowalls, Fig. 1(b). However, single crystalline nature of nanowalls structure oriented along [0001] is obvious from selected area electron diffraction (SAED) pattern, Fig. 1(c). X-rays powder diffraction pattern further endorsed the growth orientations and crystal structure of ZnO nanowalls by revealing highly intense emission peak at (2θ) 34.42° position, however no other characteristic peak is observed, Fig. 2(a). Diffraction pattern is highly corroborated with the SAED pattern endorsing single phase crystal growth orientation of ZnO nanowalls. Room temperature UV-Visible (UV-Vis) absorption spectrum of ZnO nanowalls shown in Fig. 2(b) depicts an absorption

²Pure and Applied Biochemistry, Lund University, P.O. Box 124, SE-221 00 Lund, Sweden ³Acromed Invest AB, Magistratsvägen 10, SE-226 43 Lund, Sweden

These important characteristics of nanostructures provide a motivation for the innovation of alternative nanomorphologies possessing even higher surface to volume ratio. Here, we present chemical synthesis of ZnO nanowalls and their characterization. Furthermore, ZnO nanowalls have been utilized for the fabrication of potentiometric cholesterol biosensor for routinely diagnosis holding good selectivity, sensitivity, rapid signal-transfer kinetics, molecule capturing efficiency, and stable output response. Cholesterol biosensor is prepared in two steps; first ZnO-nanowalls have been chemically synthesized on a preseeded aluminum (Al) wire of a diameter ~ 1 mm using $(5 \times 10^{-2} \text{ M})$ equimolar concentration of zinc nitrate hexahydrate and methamine at 90 °C for 2.5 h in a laboratory oven. Then, a diluted solution of ChOx by tris-HCl buffer solution $(1 \times 10^{-2} \text{ M})$ with a concentration of 500 U/ml has been applied onto ZnO nanowalls for electrostatic immobilization. Cholesterol electrolyte solutions of concentrations ranging from $1 \times 10^{-6} - 1 \times 10^{-3}$ M have been prepared from phosphate buffered saline (PBS) solution containing 1% of triton-X100.

a) Electronic mail: muhqa@itn.liu.se.

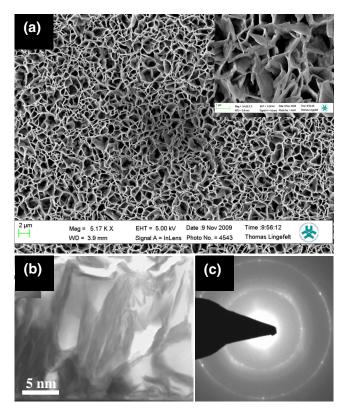


FIG. 1. (Color online) (a) Panoramic view of SEM image of ZnO nanowalls of an average thickness of 80 nm synthesized on Al wire. Insert depicts highly magnified SEM image of smooth and clear surface of the nanowalls. (b) LRTEM image of nanowalls showing clear surface without any external impurity. (c) SAED pattern image of ZnO nanowalls depicting single crystalline growth orientation.

peak near the band edge in the exciton absorption region. This peak could be assigned to the combined effect of the mutual coupling interaction and confinement of the electronhole pair along thin nanowalls of the ZnO. Moreover, the blueshifted absorption peak has been observed compared to ZnO bulk excitonic absorption peak which could be assigned to a strongly bounded exciton.

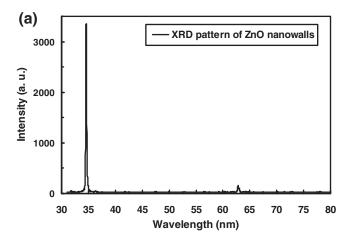
The working mechanism for the cholesterol biosensor during measurements could be explained by taking into account the dual role of ChOx where it provides not only a good specificity but also works as a catalyst to initiate the chemical reaction. The enzyme catalytic reaction between cholesterol molecule and oxygen present in the electrolyte solution produces the Δ^5 -3-ketosteroid and hydrogen peroxide as product of the chemical reaction (Refs. 19–21) [Eq. (1)],

$$\label{eq:Cholesterol} \begin{aligned} & \overset{ChO_{\chi}}{\text{Cholesterol}} + O_2 & \to \Delta^5\text{--}3\text{-ketosteroid} + H_2O_2. \end{aligned} \tag{1}$$

However, the formation of Δ^5 -3-ketosteroid as a product of the chemical reaction are highly susceptible to undergo through the spontaneous process of the isomerization of the trans double bond Δ^5 - Δ^6 of steroid ring with the intramolecular transfer of a proton from 4-6 β position producing Δ^4 - 3-ketosteroid as stable molecules [Eq. (2)],

$$\begin{array}{c} \text{Isomerisation} \\ \Delta^5\text{-}3\text{-ketosteroid} & \to & \Delta^4\text{-}3\text{-ketosteroid.} \end{array} \tag{2}$$

The proposed electrochemical reaction could be responsible for the production of the charges near the surface of the working electrode which produces an overall potential differ-



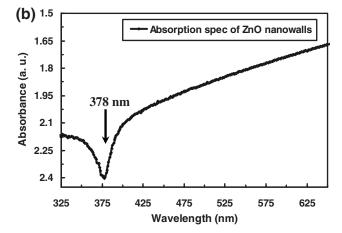
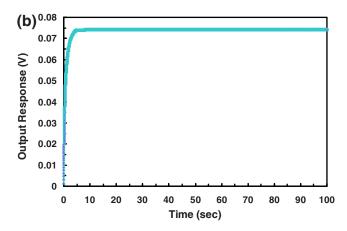


FIG. 2. (a) XRD pattern of as-grown ZnO nanowalls shows single crystal-line nature of growth orientation along [0001]. (b) UV-Vis absorption spectra of ZnO nanowalls at room temperature.

ence between cholesterol biosensor and reference electrode inside the electrolyte solution.

The electrochemical cell response EMF has been measured by utilizing two electrodes system and the resultant slope is drawn from calibrated values of EMF corresponding to each concentration cholesterol electrolyte solution ranging from $1 \times 10^{-6} - 1 \times 10^{-3}$ M. The mechanism behind the variation in the EMF values could be a result of the accumulation of different amounts of cholesterol molecules near the surface of the cholesterol biosensor against varied concentrations of cholesterol electrolyte solution. The slope of the measured EMF values by the cholesterol biosensor has been depicted as a function of the logarithmic concentration of the cholesterol electrolyte solution, Fig. 3(a). The linearity, stability, and reusability of cholesterol biosensor have been extracted by performing three consecutively repeatedexperiments by utilizing a single biosensor. The results of these experiments reveal good consistency in the calibration traces while the surfactant residuals of electrolyte solution from cholesterol biosensor have been detached by washing in PBS solution before each measurement. The linear enhancement in the EMF values against varied concentrations of cholesterol electrolyte solution could be assigned to the proportion to the number of cholesterol molecules. Additionally, ZnO nanowalls possessing high surface area to volume ratio and alternative layers of the positive and negative ions along its nonpolar plane provide a suitable microenvironment for the adsorption of the ChOx which could



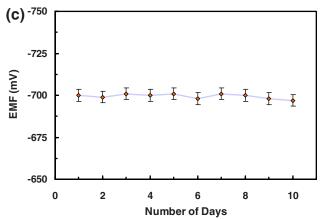


FIG. 3. (Color online) (a) EMF calibration results against a logarithmic range of cholesterol electrolyte concentrations ranging from $1\times 10^{-6}-1\times 10^{-3}$ M. (b) Output voltage response as a function of time showing good stability for cholesterol concentration of 1×10^{-4} M. (c) Results of repeated experiments for ten consecutive days using different biosensor each day showing its storages stability.

lead to improve the sensitivity of cholesterol biosensor. These important features of this configuration could play a vital role to enhance its efficacy and specificity due to the rapid signal transfer rate and biorecognition properties. The cholesterol biosensor depicts a significantly high slope value (53 mV/decade) drawn from EMF results against logarithmic concentrations of cholesterol electrolyte solution. However, the performance of cholesterol biosensor has been found to be independent from any influence of sensing area dipped into the cholesterol electrolyte solution and quantity of its volume.

Along with other features, the presented cholesterol biosensor illustrates the rapid output voltage response as a function of time. A steady-stable output signal ~5 s is found, revealing the ability of cholesterol biosensor for the prompt electrochemical signal transfer rate among the easily accessible surface of ZnO nanowalls and cholesterol molecules in the electrolyte solution, Fig. 3(b). The storage stability of cholesterol biosensor has been investigated with a series of repeated experiments for ten consecutive days to ensure its use for routinely diagnosis. However, the cholesterol biosensor has been placed at appropriate environmental conditions before and after the measurements. It is found that cholesterol biosensor holds excellent storage ability, retains its sensitivity, and reusability for long durations of time, Fig. 3(c).

Here, ZnO nanowalls with an average diameter of 80 nm have been synthesized on Al wire by utilizing a low temperature solution technique and characterized with TEM, x-ray diffraction (XRD), and UV-Vis spectrometer. Further, their conjugation with ChOx has been carried out in order to prepare a cholesterol biosensor to harvest the substantial advantages of large surface area and smooth electrical signal communication in ZnO nanowalls. Reproducibility, sensitivity, and selectivity of the biosensor have been investigated over a large dynamic logarithmic concentrations (ranging from $1 \times 10^{-6} - 1 \times 10^{-3}$ M) of cholesterol electrolyte solution and good sensitivity slope curve (~ 53 mV/decade) is achieved with rapid output response of ~ 5 s as a function of time at room temperature.

¹D. S. Fredrickson and R. I. Levy, *The Metabolic Basis of Inherited Disease* (McGraw-Hill, New York, NY, USA, 1972), p. 545.

²E. Ikonen, Nat. Rev. Mol. Cell Biol. **9**, 125 (2008).

³B. Staels, Nature (London) **417**, 699 (2002).

⁴M. Nauck, W. März, J. Jarausch, C. Cobbaert, A. Sägers, D. Bernard, J. Delanghe, G. Honauer, P. Lehmann, E. Oestrich, A. V. Eckardstein, S. Walch, H. Wieland, and G. Assmann, Clin. Chem. **43**, 1622 (1997).

⁵J. MacLachlan, A. T. Wotherspoon, R. O. Ansell, and C. J. Brooks, J. Steroid Biochem. Mol. Biol. **72**, 169 (2000).

⁶F. R. Maxfield and I. Tabas, Nature (London) **438**, 612 (2005).

⁷M. S. Samuel, J. Koshy, A. Chandran, and K. C. George, Curr. Appl. Phys. 11, 1094 (2011).

⁸J. R. Sadaf, M. Q. Israr, S. Kishwar, O. Nur, and M. Willander, Nanoscale Res. Lett. 5, 957 (2010).

⁹R. Khan, A. Kaushik, P. R. Solanki, A. A. Ansari, M. K. Pandey, and B. D. Malhotra, Anal. Chim. Acta 616, 207 (2008).

¹⁰M. Q. Israr, J. R. Sadaf, M. H. Asif, O. Nur, M. Willander, and B. Danielsson, Thin Solid Films 519, 1106 (2010).

¹¹M. H. Asif, A. Fulati, O. Nur, M. Willander, C. Brännmark, P. Strålfors, S. I. Börjesson, and F. Elinder, Appl. Phys. Lett. 95, 023703 (2009).

¹²P. R. Solanki, A. Kaushik, A. A. Ansari, and B. D. Malhotra, Appl. Phys. Lett. **94**, 143901 (2009).

¹³S. M. Al-Hilli, M. Willander, A. Öst, and P. Strålfors, J. Appl. Phys. **102**, 084304 (2007).

¹⁴B. Piro, V.-A. Do, L. A. Le, M. Hedayatullah, and M. C. Pham, J. Elec-

troanal. Chem. **486**, 133 (2000). ¹⁵H. Wang, Sens. Actuators B **56**, 22 (1999).

¹⁶Q. Yang, Sens. Actuators B **46**, 249 (1998).

¹⁷E. Tamiya, Y. Sugiura, A. Akiyama, and I. Karube, Ann. N.Y. Acad. Sci. **613**, 396 (1990).

¹⁸Z. Yang, X. Zong, Z. Ye, B. Zhao, Q. Wang, and P. Wang, Biomaterials 31, 7534 (2010).

¹⁹J. Besombes, Anal. Chim. Acta **317**, 275 (1995).

²⁰J. Motonaka and L. R. Faulkner, Anal. Chem. **65**, 3258 (1993).

²¹L. Charpentier, Anal. Chim. Acta **318**, 89 (1995).